

Mid-IR Observations of Mira Circumstellar Environment

Massimo Marengo, Margarita Karovska, Giovanni G. Fazio, Joseph L. Hora

Harvard-Smithsonian Center for Astrophysics, 60 Garden St., Cambridge, MA 02138

`mmarengo@cfa.harvard.edu`

William F. Hoffmann

Steward Observatory, University of Arizona, 933 North Cherry Avenue, Tucson, AZ 85721-0065

Aditya Dayal

KLA-Tencor Corporation, 160 Rio Nobles, San Jose, CA 94134

and

Lynne K. Deutsch

Department of Astronomy, CAS 519, Boston University, 725 Commonwealth Ave., Boston, MA 02215

ABSTRACT

This paper presents results from high-angular resolution mid-IR imaging of the Mira AB circumbinary environment using the MIRAC3 camera at the NASA Infrared Telescope Facility (IRTF). We resolved the dusty circumstellar envelope at 9.8, 11.7 and 18 μm around Mira A (*o* Ceti), and measured the size of the extended emission. Strong deviations from spherical symmetry are detected in the images of Mira AB system, including possible dust clumps in the direction of the companion (Mira B). These observations suggest that Mira B plays an active role in shaping the morphology of the circumstellar environment of Mira A as it evolves toward the Planetary Nebula phase.

Subject headings: circumstellar matter — infrared: stars — binaries: close — stars: individual (*o* Ceti)

1. Introduction

Mira A (*o* Ceti, Mira) is a cool pulsating giant of M2-7 III spectral type, with a mass comparable to our Sun and a diameter of several hundred solar radii. Prototype of the Mira-type class of Long Period Variables (LPVs), it has a period of 332d during which its brightness changes by several magnitudes in the optical. Mira has a hot companion (Mira B) at an angular distance of $\sim 0.6''$.

The companion is probably a white dwarf accreting from Mira’s wind (Reimers & Cassatella 1985; Karovska et al. 1997).

Recent HST observations detected significant asymmetries in the giant’s atmosphere and found evidence for possible interaction with its companion. The HST Faint Object Camera (FOC) optical images showed that Mira A atmosphere is elongated in the direction of 175° with an apparent size of 56 mas. HST UV images showed a “hook-like” structure extending eastward from Mira A photosphere towards Mira B (NASA and STScI Press Release 1997; Karovska et al. 1997). These results suggest that the companion may have an important role in shaping the circumstellar environment of the system.

Mira A is losing mass via a strong dust driven wind, at the rate of $\sim 5 \cdot 10^{-7} M_\odot \text{ yr}^{-1}$ (see Loup et al. 1993, and references therein). As a consequence, the star is surrounded by an extended circumstellar envelope of gas and dust. Observations of Mira A molecular envelope at radio wavelengths show deviations from spherical symmetry (see e.g. Planesas et al. 1990; Josselin et al. 2000). The dust is revealed via its strong infrared excess (IRAS 1986; Gezari 1993), dominated by an emission feature at $10 \mu\text{m}$ which identify an O-rich composition (Monnier et al. 1998). Evidence for spatially extended emission from Mira circumstellar dust was first obtained by Bauer & Stencel (1994), analyzing the IRAS satellite data at $60 \mu\text{m}$. More recently, mid-IR observations have been performed at $11 \mu\text{m}$ with the ISI interferometer, probing the dust distribution at a smaller spatial scale. By fitting the observed visibilities with models, Lopez et al. (1997) inferred the presence of asymmetries and inhomogeneities in Mira’s dust envelope.

Mira-type stars are in the Asymptotic Giant Branch (AGB) phase, and are among the precursors of Planetary Nebulae (see Habing 1990, for a review). The dynamical evolution of AGB circumstellar envelopes is largely controlled by the dust component, which mediates the momentum transfer from the radiation field to the molecular gas. Mapping the spatial distribution of the dust grains in the Mira AB circumbinary environment is thus necessary to understand the future evolution of the system towards the PN phase, and the dynamics of the interaction between its two stellar components.

We present here the first sub-arcsecond mid-IR images of Mira A circumstellar environment which map the 2-dimensional distribution of the dust emission. The observations and the techniques for data acquisition and reduction are presented in the next section. The results are shown in section 3, and discussed in relation to other available observations and models.

2. Observations and Data Reductions

The observations were performed on September 22, 1999 (JD2451444) when the source was at light curve phase 0.7, close to minimum luminosity (AAVSO). We used the mid-IR camera MIRAC3 (Hoffmann et al. 1998), mounted at the 3.0m NASA Infrared Telescope Facility (IRTF). MIRAC3 uses a Boeing HF16 128×128 Si:As blocked impurity band detector. On the IRTF MIRAC3 has a

plate scale of $0.34 \text{ arcsec pix}^{-1}$, providing a total field of view of $42'' \times 42''$. This pixel scale ensures Nyquist sampling of the diffraction-limited Point Spread Function (PSF).

We obtained images of Mira AB in MIRAC3 9.8, 11.7 and $18.0 \mu\text{m}$ 10% passband filters, with a total on-source integration time of 1600 s at each wavelength. The reference star α Tau was observed when transiting at a similar airmass of the source, to provide flux and PSF calibration.

We used a standard nodding and chopping technique to remove the background signal, dithering the source on the array to obtain sub-sampling of the PSF. The chop frequency was set to 2 Hz, with a throw of $20''$ in the north-south direction. The nod throw was also set to $20''$, but in the east-west direction, in order to have all four chop-nod beams inside the field of view of the array. Each individual nod cycle required 10 s on-source integration, and the procedure was repeated for as many cycles as needed to obtain the requested total integration time.

The data was analyzed by first subtracting the chop-on from the chop-off frames for both nodding beams. The two images thus obtained were then subtracted one from the other, in order to get a single frame in which the source appears in all four beams (two negative and two positive). We then applied a gain matrix, derived from images of the dome (high intensity uniform background) and the sky (low intensity uniform background), to flat field the chop-nodded image.

This procedure was repeated for each of the nodding cycles for which the source was observed. A final high signal-to-noise ratio cumulative image was then obtained by co-adding together all the beams, each re-centered and shifted on the source centroid. The last bit of co-adding was performed on a sub-pixel grid having the size of one-fifth (9.8 and $11.7 \mu\text{m}$ images) or one-third ($18.0 \mu\text{m}$ image) of the original MIRAC3 pixels, thus providing a final pixel scale of 0.068 and $0.114 \text{ arcsec pix}^{-1}$ respectively. A mask file to block out the effects of bad pixels and field vignetting was also created and applied at this stage, preventing individual rejected pixels from contributing to the final image. The same observing and reduction procedure was also used for the reference star, to ensure a uniform treatment of the source and the standard.

3. Results and Discussion

3.1. Source photometry

We first estimated the brightness of Mira AB using the multi-wavelength co-added images. The aperture photometry at the three observed wavelengths yields $\sim 2710 \text{ Jy}$ at $9.8 \mu\text{m}$, $\sim 2170 \text{ Jy}$ at $11.7 \mu\text{m}$ and $\sim 2020 \text{ Jy}$ at $18.0 \mu\text{m}$ (see Table 1). Photometric errors are of the order of 5% at 9.8 and $11.7 \mu\text{m}$ and 8% at $18.0 \mu\text{m}$.

Our measurements are consistent with the published mid-IR fluxes of the source (Gezari 1993) which are in the range $1300\text{--}5400 \text{ Jy}$ at $\sim 10 \mu\text{m}$, $1500\text{--}5500 \text{ Jy}$ at $11\text{--}12 \mu\text{m}$ and $1100\text{--}2800 \text{ Jy}$ around $18 \mu\text{m}$. This wide spread, in part due to the large uncertainties of the published data, is

a consequence of the source long period variability, which is still present at infrared wavelengths. Note that, in the mid-IR, only a small fraction of the overall luminosity is contributed by Mira A stellar flux, due to the greater brightness of the dust envelope. The observed infrared variability is thus affected by the changes in the physical and thermodynamical status of the circumstellar dust.

3.2. Size of Mira’s dust envelope

Our images of Mira AB at 9.8, 11.7 and 18.0 μm indicate that the dusty envelope is spatially resolved at all observed wavelengths. This is shown in Figure 1, which plots the azimuthal averages of the source and reference (radial profiles), normalized at the same peak value. In all panels the source profile has a larger FWHM than the reference star (assumed to be a point source), which is a clear indication of spatial extension. The measured FWHM are listed in Table 1.

We estimated the apparent size of Mira AB envelope as a function of wavelength by convolving the reference star profile with a gaussian model of Mira A envelope, and then fitting to the source radial profile. We obtained a FWHM of 0.34”, 0.35” and 0.86” for the best fit gaussian model at 9.8, 11.7 and 18.0 μm respectively. As expected, the apparent sizes of Mira are almost the same at 9.8 and 11.7 μm . Mira A envelope is significantly larger at 18 μm . We obtained very similar results using deconvolved images described in the next section. Using a Hipparcos measured distance of 128 pc (Perryman et al. 1997) we estimate the apparent spatial scale of Mira A dust envelope from 50 AU (at 10 μm) to 100 AU at 18 μm .

The measured apparent sizes of the dust envelope are 10-20 times larger then the apparent size of Mira A photosphere. For example, the mid-infrared observations using the ISI interferometer resolved Mira A stellar photosphere, measuring a uniform disk diameter of 47.8 mas (Weiner et al. 2000).

The larger size of the 18 μm envelope can be explained on the bases of the radiative transfer properties of AGB envelopes, which in general have a radial thermal structure that can be approximated with a power-law $T \propto r^{-0.4}$ (Ivezić & Elitzur 1997). Since the peak of emission for the dust radiation at a certain wavelength is inversely proportional to the grain temperature (Wien’s law), one should expect $T_{18\mu\text{m}}/T_{11.7\mu\text{m}} \simeq 0.65$. This means that the size of the region where most of the 18 μm flux is produced should be $r_{18\mu\text{m}} \simeq 2.9 r_{10\mu\text{m}}$. This factor is similar to the measured ratio between the FWHM of the 18.0 and 11.7 μm deconvolved images (~ 2.5), and much larger than the PSF spread due to the telescope resolving power (proportional to λ , e.g. ~ 1.5). Note that this calculation is only a rough estimate for the real size of the envelope. Better estimates can be obtained using models including physical parameters such as the dust condensation radius. This requires a simultaneous fitting of the radial intensity profile and the source spectral energy distribution, which allows derivation of the envelope optical depth τ_V and the inner shell temperature T_1 (Marengo et al. 2001). Results using these models will be presented in a separate paper.

3.3. Envelope asymmetries

Our multi-wavelength direct mid-IR images show asymmetries that aren't seen in the images of the reference star taken with the same filters. We confirmed the presence of significant departures from spherical symmetry in Mira's dust envelope by performing deconvolution using the Richardson-Lucy method (Richardson 1972; Lucy 1974). The images at 9.8 and 11.7 μm were deconvolved with the corresponding reference star images used as PSFs. This technique was not applied to the 18.0 μm image, due to the lower S/N of the source/reference pair.

The deconvolved images are similar at 9.8 and 11.7 μm , as shown in Figure 2. They show that the spatial distribution of the dust in Mira A circumstellar environment is clearly not spherical. Two dominant asymmetries are detected in the images: one with a major axis position angle of 175° , and another at a position angle of approximately 110° .

The first asymmetry is in the same direction as the asymmetry in the Mira A TiO envelope observed with the HST in 1995 (Karovska et al. 1997), but its apparent size is roughly ten times larger than the one measured in the HST images. Near-IR images obtained in the JHK bands by Cruzalèbes et al. (1998) also show a N-S elongated shape, which has been interpreted as scattered light from dust. The observed asymmetries could be due to an asymmetric outflow, as suggested by Planesas et al. (1990) and Josselin et al. (2000).

The second dominant asymmetry in Mira AB mid-IR images is in the direction of the companion. This is in agreement with earlier mid-IR observations suggesting the presence of an eastward asymmetry (Lopez et al. 1997; Meixner 2000). Figure 2 shows the location of the companion as observed by the HST in the late 1995 (Karovska et al. 1997). We do not expect that the position angle and the separation of the companion have changed substantially since 1995, because of its long orbital period of several hundred years (Baize 1980). Our images indicate that the companion is embedded in the elongated dust envelope of Mira A. Because of the limited angular resolution in these observations we cannot determine if the asymmetry is due to a second unresolved clump located in the vicinity of the companion, or is a continuous extension of the Mira A dust envelope toward the companion.

Furthermore, a fainter clump slightly above the noise level is resolved at a distance of 1.1'' from the main source, with a position angle 115° . Its brightness is $\sim 14.0 \pm 1.5$ Jy at 9.8 μm and $\sim 11.0 \pm 1.0$ Jy at 11.7 μm , which is a factor ~ 200 fainter than the main source. We estimate a color temperature of 390 ± 100 K, obtained by black body fitting of the clump brightness at the two observed wavelengths. The presence of dust clumps has been suggested by interferometric observations using the ISI 11 μm visibilities by Lopez et al. (1997). Their "Clump 3" model, in particular, invokes the presence of dust clumps with position angle 120° , which may thus be associated with our observed structures.

The mid-IR observations of Mira AB system indicate that the shape of Mira A circumstellar envelope may be directly influenced by the presence of the companion orbiting the main AGB

mass losing star. Hydrodynamic models in dusty winds of close binary systems (Mastrodemos & Morris 1999) predict the formation of spiral shocks in the orbital plane, which trail and follow the secondary star. The structures observed in the mid-IR may be related to this kind of phenomenon. However, the interpretation of the observed geometry is still open, given that the dynamics of the interactions between the two components of close binary systems is not well understood.

4. Conclusions

Our mid-IR images of Mira AB dust envelope show significant departures from spherical symmetry. They also indicate that the overall distribution of the circumstellar dust is affected by the presence of a companion. Given the role of dust in shaping the future dynamical evolution of the system, these observations not only give a better characterization of the geometry of the Mira AB binary system, but may also contribute to a better understanding of the formation of asymmetric PN.

Many details of the transition from AGB to PNs cannot be explained on the basis of the spherically symmetric “interacting stellar winds” theory (Kwok et al. 1978) which defines the general framework of PN formation. High resolution HST images of PNs reveal a general absence of spherical symmetry, in favor of bipolar structures enriched by a multitude of micro-structures (jets, clumps, “fliers”, etc. . .). Optical and mid-IR images of post-AGB and pre-PN (Sahai et al. 1998; Meixner et al. 1999; Ueta et al. 2000) show envelope asymmetries already present before the onset of the PN phase. How these structures evolve is unknown. The results of our IR observations show that Mira AB offers the possibility of observing the beginning of this process.

We thank the IRTF staff for their outstanding support. M. K. is a member of the Chandra Science Center, which is operated under contract NAS8-39073, and is partially supported by NASA. We also thanks the referee for his useful comments.

REFERENCES

- Baize, P. 1980, *A&AS* 39, 83
- Bauer, W.H., Stencel, R.E. 1994, *AJ* 107, 223
- Cruzalèbes, P., Lopez, B., Bester, M., Gendron, E., Sams, B. 1998, *A&A* 338, 132
- Gezari, D.Y. 1993, *Catalog of Infrared Observations*, NASA publ.
- Habing, H.J. 1990, in proc. “From Miras to Planetary Nebulae: Which Path for Stellar Evolution?”, eds. M.O. Mennessier, A. Omont, p. 16
- Hoffmann, W.F., Hora, J.L., Fazio, G.G., Deutsch, L.K., Dayal, A. 1998, *Proc. SPIE* 3354, 647
- IRAS Catalogues and Atlases, *Catalogue of Point Sources*, IRAS Science Team 1986, IPAC
- Ivezić, Ž, Elitzur, M. 1997, *MNRAS* 287, 799
- Josselin, E., Mauron, N., Planesas, P., Bachiller, R. 2000, *A&A* 362, 255
- Karovska, M., Hack, W., Raymond, J., Guinan, E. 1997, *ApJ* 482, L175
- Kwok, S., Purton, C.R., Fitzgerald, P.M. 1978, *ApJ* 219, 125
- Lopez, B., Danchi, W.C. Bester, M., Hale, D.D.S., Lipman, E.A., Monnier, J.D., Tuthill, P.G., Townes, C.H., Degiacomi, C.G., Geballe, T.R., Greenhill, L.J., Cruzalèbes, P., Lefèvre, J., Mékarnia, D., Mattei, J.A., Nishimoto, D., Kervin, P.W. 1997, *ApJ* 488, 807
- Loup, C., Forveille, T., Omont, A., Paul, J.F. 1993, *A&AS* 99, 291
- Lucy, L.B. 1974, *AJ* 79, 745
- Marengo, M., Ivezić, Ž., Knapp, G.R 2001, *MNRAS* 324, 1117
- Mastrodemos, N., Morris, M. 1999, *ApJ* 523, 357
- Meixner, M. 2000, private communication.
- Meixner, M., Ueta, T., Dayal, A., Hora, J.L., Fazio, G., Hrivnak, B.J., Skinner, C.J., Hoffmann, W.F., Deutsch, L.K. 1999, *ApJS* 122, 221
- Monnier, J.D., Geballe, T.R., Danchi, W.C. 1998, *ApJ* 502, 833
- NASA and STScI Press Release 1997, STScI-PRC97-26
- Perryman, M.A.C., Lindegren, L., Kovalevsky, J., Hog, E., Bastian, U., Bernacca, P.L., Creze, M., Donati, F., Grenon, M., Grewing, M., van Leeuwen, F., van der Marel, H., Mignard, F., Murray, C.A., Le Poole, R.S., Schrijver, H., Turon, C., Arenou, F., Froeschle, M., Petersen, C.S. 1997, *A&A* 323, 49

Reimers, D., Cassatella, A. 1985, ApJ 297, 275

Richardson, W.H. 1972, J. Opt. Soc. Am. 62, 55

Planesas, P., Kenney, J.D.P., Bachiller, R., 1990, ApJ 364, L9

Sahai, R., Trauger, J.Y., Watson, A.M., Stapelfeld, K.R., Hester, J.J., Burrows, C.J., Ballister, G.E., Clarke, J.T., Crisp, D., Evans, R.W., Gallagher, J.S.III, Griffiths, R.E. Hoessel, J.G., Holtzman, J.A., Mould, J.R., Scowen, P.A., Westphal, J.A. 1998, ApJ 493, 301

Ueta, T., Meixner, M., Bobrowsky, M. 2000, ApJ 528, 861

Weiner, J., Danchi, W.C., Hale, D.D.S., McMahon, J., Townes, C.H., Monnier, J.D., Tuthill, P.G. 2000, ApJ 544, 1097

TABLE 1
MID-IR PHOTOMETRY AND ANGULAR SIZE

Wavelength	Photometry	FWHM radial average profile source	reference
9.8 μm	2710 (\pm 135) Jy	1.05''	0.97''
11.7 μm	2170 (\pm 110) Jy	1.08''	1.01''
18.0 μm	2020 (\pm 270) Jy	1.56''	1.32''

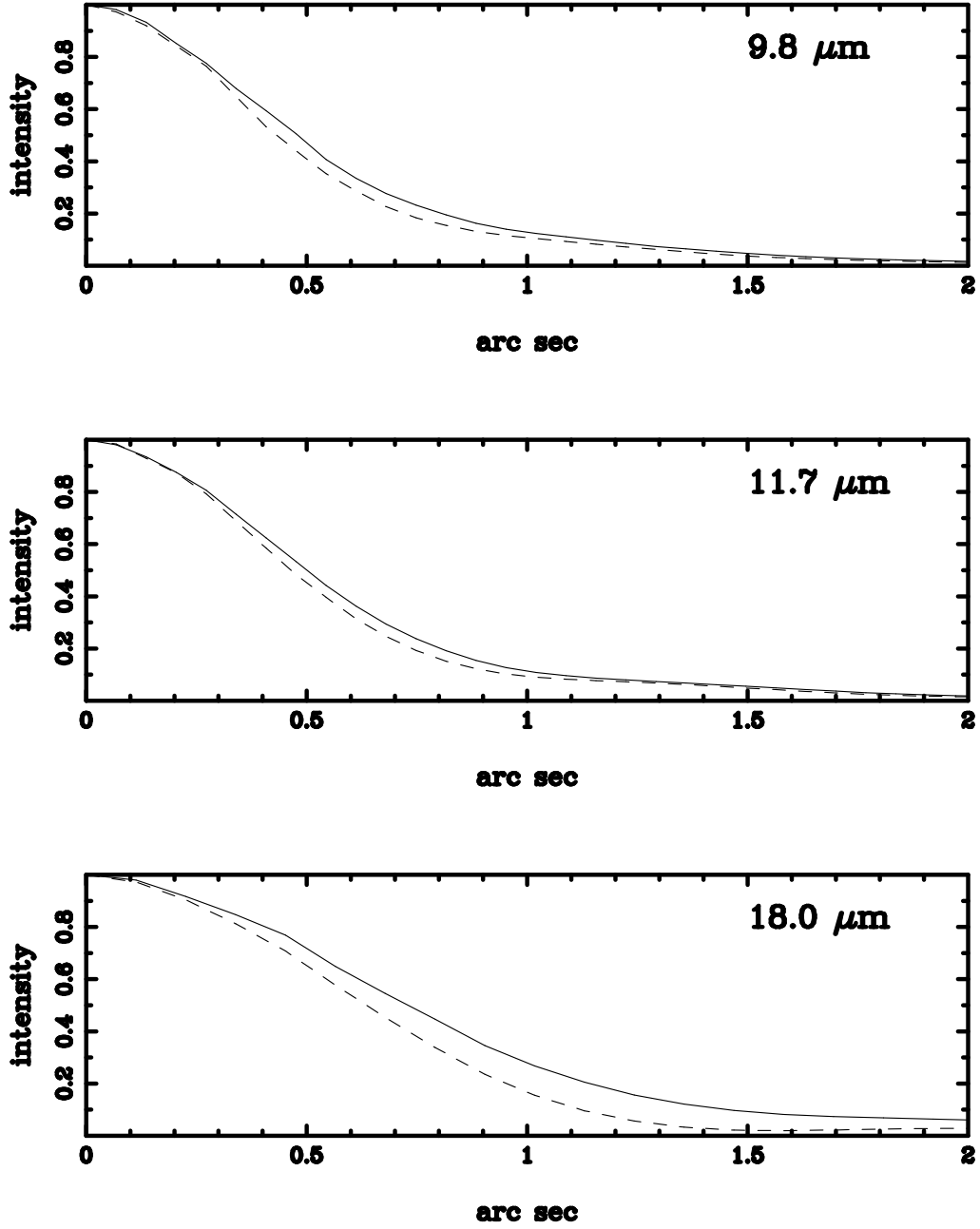


Figure 1. Radial profiles of Mira AB image (solid line) and of the reference image (dashed line) at 9.8, 11.7 and 18.0 μm .

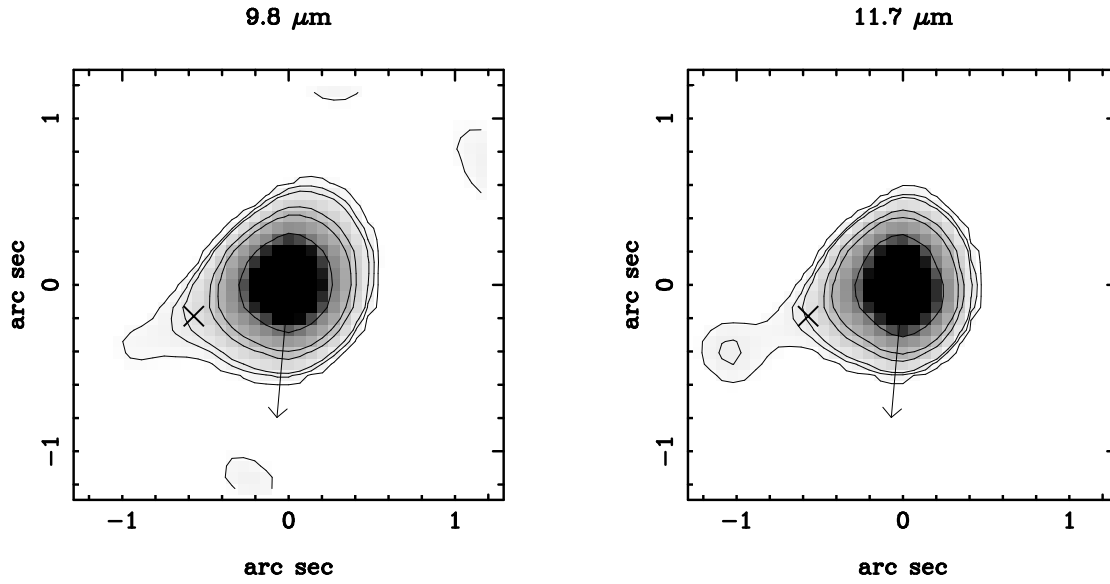


Figure 2. Deconvolved images of Mira AB at 9.8 and 11.7 μm . North is up and West is right. The location of Mira B, as observed by the HST in 1995, is marked by a cross; the arrow indicates the orientation of the dominant asymmetry in the 1995 HST image of Mira A (Karovska et al. 1997). The contours are plotted for 0.001, 0.005, 0.01, 0.05, 0.1 and 0.5 of the maximum flux density level.